Development of Wireless Sensor Network to Detect Lameness in Dairy Cows

by

Thanh Nha Nguyen

Submitted to the Department of Mechanical Engineering
in partial fulfillment of the requirements for the degree of

Master of Science in Mechanical Engineering

at the

MASSACHUSETTS INSTITUTE OF TECHNOLOGY

May 2022

Author . . . .
Department of Mechanical Engineering
May 12, 2022

Certified by . . . .
Ian Hunter
George N. Hatsopoulos Professor in Thermodynamics
Thesis Supervisor

Accepted by . . . .
Nicolas Hadjiconstantinou
Chairman, Department Committee on Graduate Theses

Development of Wireless Sensor Network to Detect Lameness in Dairy Cows

by

Thanh Nha Nguyen

Submitted to the Department of Mechanical Engineering
on May 12, 2022, in partial fulfillment of the
requirements for the degree of
Master of Science in Mechanical Engineering

Abstract

Bovine mastitis, lameness, and calving are three major problems in the dairy farming industry. They lead to economic losses and decreased animal welfare. With the industrialization of dairy farms, these problems are magnified due to the lack of skilled labor. This work introduces a design for a wireless sensor network to automate the health monitoring of every cow on a farm. Through the constant monitoring of health statistics, we can make a prediction about the early onset of mastitis, lameness, and calving and therefore reducing the burdens on the farmers. The network architecture is designed to accommodate a large number of cows (1000s) and the size of dairy farms (area >1500000 m^2) by combining a short-range and a long-range communication protocol (Bluetooth Low Energy (BLE) and LoRa). This work also explores the use of IMUs for lameness detection in walking gaits. Taking advantage of the holonomic constraints of animal limbs, Principal Component Analysis is able to compress the highly correlated data of locomotion into a smaller dimension in which abnormal gaits can be differentiated.

Thesis Supervisor: Ian Hunter
Title: George N. Hatsopoulos Professor in Thermodynamics

Acknowledgments

I want to first give thanks to Professor Ian Hunter for providing a wonderful environment to learn and explore. The freedom to take any path in the BioInstrumentation Lab has been very valuable for me. On that note, I also want to thank the other students within the lab: Kristan Hilby, Ryan Poon, Marc-Andre Begin, Annie Chen, Vineet Padia, Michael Aling, Zhong Huang, and Peter Morice. Your continual company through the COVID-19 season has done wonders for my mental health. I'm grateful for all the support and advice I have received from everyone. I would also like to thank Dr. Cathy Hogan for her vast experience in biology research. Without her help, I would be very lost in planning and executing animal experiments. Special thanks to Ms. Shibani Joshi for being a reliable source of logistical help and administrative knowledge.

To my friends at Imobilare and The Flavor Continues, thank you for providing a creative outlet outside of my lab. My time with you guys has led me to so many new ideas here at work.

Finally, I would like to thank my family - my sister, Truc Nguyen, and my mom, Thi Tran. You guys are always there for me.

This research was supported in part by Fonterra Co-operative Group Limited.

Contents

List of Figures

Chapter 1

Introduction

1.1 Background

For a typical pasture-based dairy farm in New Zealand, the farm has an area of 1500000 m^2 and has an average herd size of 440 cows [21]. With such a large area and amount of animals to take care of, individual care cannot be provided for every animal. Plaguing the dairy farming industry are a few persistent and common diseases. As dairy cows become sick, they become less productive and as a result, the dairy farm loses out economically. Some of these common and yet curable issues are mastitis, lameness, and calving.

Bovine mastitis is the cause of the largest economic loss in dairy farming [19]. Mastitis is an inflammatory response at the udder due to physical injuries or infections [9]. Due to the mammary tissue damage, the disease causes a decrease in milk production. The disease can be classified with a severity level of clinical and subclinical. In clinical cases, the symptoms are easy to detect: red and swollen udder, fever, and watery milk [9]. In severe cases, it can be fatal. However, more insidiously is the subclinical case, there are no visible signs in the udder or milk, but there is a reduction in milk yield. Overall, the subclinical cases account for more financial damage for the farms [9].

Lameness is currently one of the primary difficulties of the cattle industry. The disease includes any conditions on the foot or leg that leads to abnormal walking gaits. It has a serious impact on fertility and milk yield [2]. Without early treatment, the conditions will lead to infection of the bones, tendons, and ligaments. In late stages, the infections will lead to sepsis and eventually culling of the cow [19]. As cows become immobile and lie down more, the cow becomes more susceptible to mastitis. It is estimated that a typical UK dairy herd loses £7,499.30 per year to this issue. Ideally, medical intervention is required to fix the condition. However, with the increased industrialization of the dairy farming industry, individual hands-on treatment per cow is limited. Currently, the only way to detect lameness is through a visual inspection done with a trained professional [19]. As such, early detection of the issue is very difficult on a large farm.

Calving is a critical period in a cow's and calf's life as both animals become at high risk for death. Complications during such a period will lead to morbidity or death [8]. One example complication is Dystocia, awkward positioning of the fetus leading to a lengthening birthing process. It increases the likelihood of stillborn and the health of the newborn calf. For any cattle farm, reproduction is an important process for profitability. Any inefficiencies will reduce economic output. Close monitoring of the parturition process can alleviate the complications. Traditionally, an experienced farmer is needed to make careful observations of the farm to find the moment of calving and provide assistance [8]. However, the industrial scale of modern farms naturally leads to a lack of skilled labor needed for this process.

1.2 Objectives

For all three of these issues, the common theme is the lack of manpower to provide the necessary healthcare for the animals. The goal of this thesis is to introduce modern technology into the dairy farming industry. With constant and automated health monitoring of every cow on a farm, we can reduce the burdens of these common issues. In bovine mastitis, with more health signals, we could predict the subclinical cases by observing for symptoms not easily viewed by a human. The constant monitoring of health statistics can pick up deviations from a baseline level of health. Instead of using a subjective judgment for lameness, we can monitor the walking gaits of every cow in the herd. Early lameness levels can be detected and will lead to easier and cheaper treatment. Farmers can be notified of calving behaviors without being in the field. From a central server, trained professionals can be notified of a parturition event and be sent to assist.

This thesis introduces a novel wireless sensor network that combines a short-range and a long-range communication protocol. Through this combination, the sensor network can be utilized to work in any size of a dairy farm. The network is flexible enough to handle any type of health metrics. While at the same time, the sensors are low maintenance. Once installed, upkeep is needed only once a year. Finally, the thesis looks at how this network can be used to perform lameness detection with Inertial Measurement Units.

Chapter 2

Literature Review

2.1 Wireless Technology

2.1.1 Bluetooth Low Energy

Bluetooth Low Energy (BLE) is a wireless technology developed by the Bluetooth Special Interest Group (SIG) as an additional capability of Bluetooth introduced in the Bluetooth 4.0 update. BLE is designed to be a low-power short-range communication protocol [12]. In contrast to other low-power wireless solutions like ZigBee, 6LoWPAN, or Z-Wave, BLE provides a single-hop communication solution as opposed to multi-hop [11]. In exchange, BLE is capable of 1000 kbps bitrate compared to the 250 kbps bitrate of the other low-power solutions [11].

The BLE protocol operates on the 2.4 GHz band with 40 channels each with 2 MHz channel spacing. Three channels are defined to be advertising channels while the rest are used as data channels. Within the 37 data channels, an adaptive frequency hopping mechanism is used to minimize interference by selecting the most optimal channel for a given communication interval. The protocol has two different roles defined, Central and Peripheral. A Central can simultaneously connect to multiple Peripherals, but each Peripheral can only communicate with one Central. Thus, the network protocol only allows a star topology network.

One defining characteristic of BLE over the original Bluetooth specification is the usage of Generic Attribute (GATT). GATT is a predefined data structure composed of nested objects: Profiles, Services, and Characteristics. Once a dedicated connection, GATT defines the data packet that is passed between the two devices. The Bluetooth SIG has created many predefined GATT profiles like the Asset Tracking Profile, Blood Pressure Profile, Automation IO Profile, and Environmental Sensing Profile. By having open standards regarding different application profiles, BLE devices made by different users can easily interoperate. For example, an application user can use the Environmental Sensing Profile as their GATT profile. Anyone else can interpret the data packages once a connection is made thanks to the open standard. The application user can still choose to define their own custom GATT profile tailor-made to their use case should it need be.

Figure 2-1: Nested Structure of GATT data structure

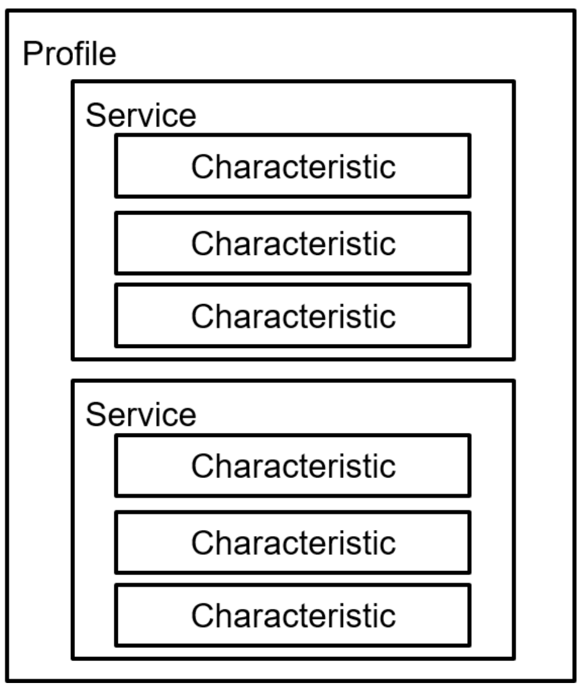

With an empirical power measurement, a BLE transmission event sending 31 bytes of data at a distance of 0.5 m consumes 142 μJ [17]. Using a 0.76J battery, a typical coin cell battery, a Peripheral device sending data every 3 seconds, in theory, can last for 2 years [11]. These results make BLE an ideal short-range communication protocol.

2.1.2 Long Range (LoRa)

Low-Power Wide-Area Network (LPWAN) is a type of wireless communication design for long-range communication (over 10 kilometers in a rural environment) at a low bit rate (on the order of 1 kbps). LoRa is one such protocol operating in the 915 MHz band [15]. Developed by Semtech, the proprietary protocol uses Chirp Spread Spectrum as a modulation scheme [6]. One advantage of this modulation is that the data size does not affect power consumption. The energy needed for transmission is only dependent on time on-air (T) and antenna output power. The three main parameters influencing the time on-air are bandwidth, spreading factor, and code rate.

Figure 2-2: Example Chirping Signal from 1 to 10 Hz

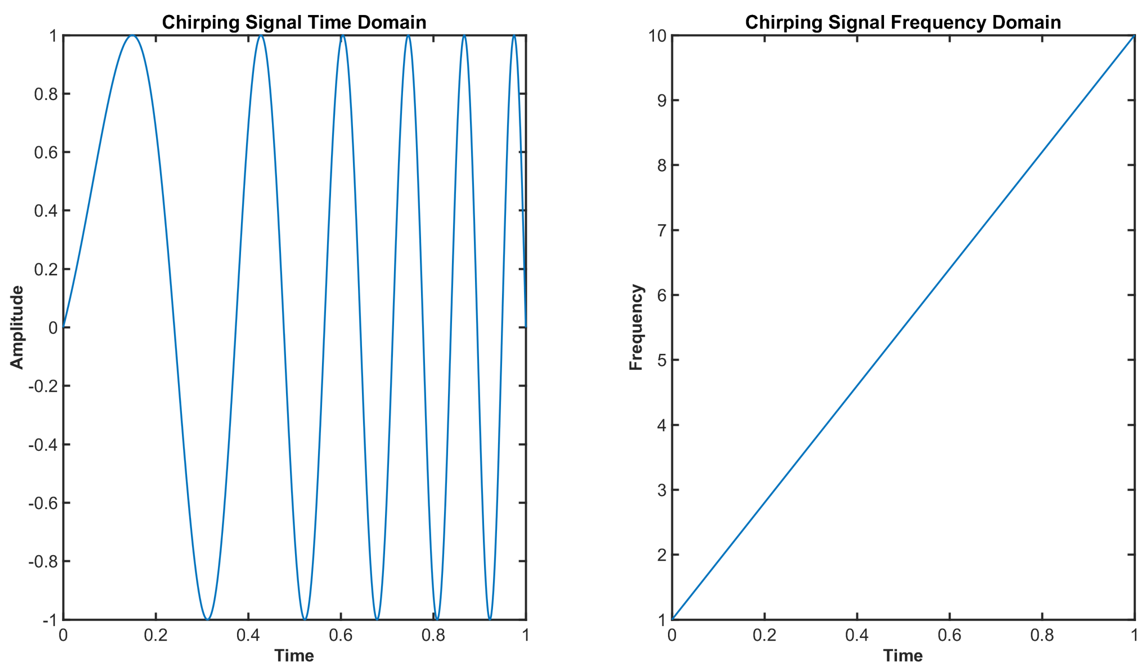

To understand this modulation scheme, let's look at one example chirping signal and how data can be encoded in it. In Figure 2-2, we can observe a chirping signal that changes from 1 Hz to 10 Hz over 1 second. To encode digital data onto this chirping signal, we shift the starting frequency of the signal and loop to the lower frequency once we hit the upper-frequency limit. For example, we can start the signal at 2 Hz, increase it to 10 Hz, then shift to 1 Hz again then ramp to 2 Hz. For each shift, we take that signal as an encode for a specific value.

Figure 2-3: Different modulated data on the same chirping signal

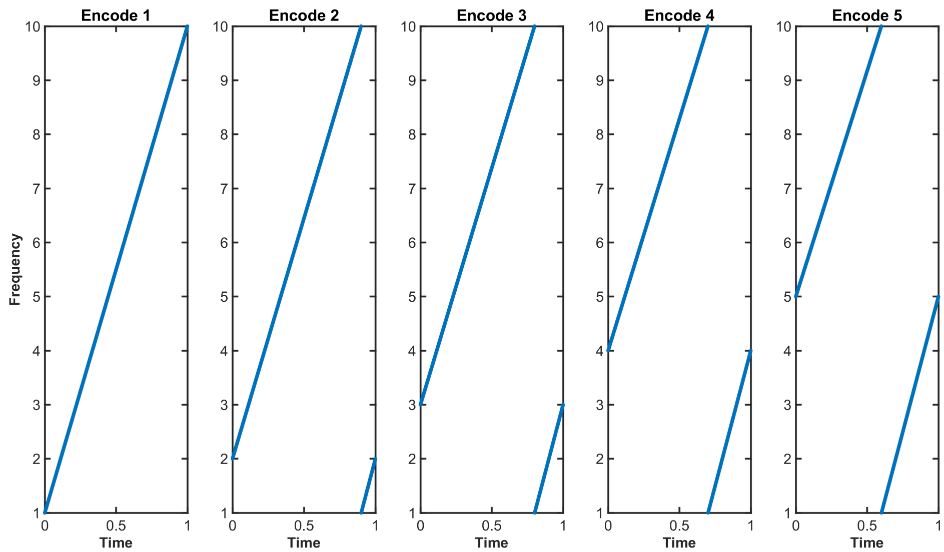

In LoRa, each transmission symbol is modulated on one chirping signal in the interval $(f_0 - B/2 f_0 + B/2)$, where f_0 is the center frequency (915 MHz in the US), and B is the bandwidth of the signal. LoRa allows for either 125, 250, or 500 kHz as the bandwidth. By selecting a larger bandwidth, we can send one chirping signal faster and therefore higher data rate. However, the trade-off is for a lower transmission range. The spreading factor, SF, determines how fine the frequency shift is and therefore the size of the transmission symbol. In LoRa, the amount of shift per encoding (or chips) is calculated to be 2^{SF}. To accommodate for a higher resolution of chips, the time it takes to complete one chirp increases. For each increase in SF, the chirp duration doubles. Increasing SF decreases the overall data rate but would increase the receiver sensitivity and therefore transmission range. Code rate defines the amount of error correction data added to the symbols to increase receiver sensitivity. A higher code rate (CR) would reduce the data rate but would increase sensitivity. The relationship can be summarized with the following equations (R_b is the data rate in bits/sec):

$$T = 2^{SF}/B,$$

$$R_b = SF\frac{\frac{4}{4+CR}}{\frac{2^{SF}}{BW}}.$$

With all of these parameters, LoRa can be adjusted to have 300 bit/s up to 5.5 kbit/s data rate [6]. One complication operating LoRa in the US is the FCC limitation of Time on Air of 400 ms. For each increase in SF value, the Time on Air doubles, so in practicality, SF is maxed out at 10 for operating in the US. In empirical measurements, a LoRa end-device consumes 2 mJ to send 10 bytes of data using SF 7 and 3 dBm of output power [6].

LoRa is designed to transmit sensor data to a central server. This is accomplished by the use of gateways that are connected to the internet. Each LoRa end-devices send information to a LoRa gateway which will forward data to an internet server. Results show that given a 3-channels gateway, 5000 end-devices each sending 180 bytes per hour can be supported [1].

2.2 Analysis of Gait

2.2.1 Current Method for Lameness Detection

Lameness is a symptom caused by a variety of diseases and injuries [23]. Identifying the underlying disease is valuable information for management. Currently, the diversity in methodologies, sample size, and high variance in reported incidence rate complicate data acquisition and analysis [2]. At this time, detection is most often based on a visual evaluation using subjective locomotion scoring to recognize changes in gait patterns. The scale assesses changes in stride, body poses, and abnormal position of the back resulting in diversity in lameness scoring [3] [24]. The table below outlines one such subjective visual scoring method [24].

Lameness Score	Walking Speed	Stride	Weight Bearing	Head	Backline
0 - Normal	Normal	Long and even	Even bearing	Below backline	Straight
1 - Light Lameness	Normal	Uneven rhythm	Even bearing	Slightly bob	Mildly arched when walking
2 - Lame	Slow. May stop when turning	Shortened Stride. Rear-foot miss front foot placement	Uneven	Bob up and down when walking	Often arched
3 - Severe Lameness	Very Slow. Cannot keep up with herd	Shorten and uneven stride	Barely stand on the lame leg	Large motion when walking	Arched while standing and walking

2.2.2 Usage of Sensors for Gait Analysis

Objective quantification of lameness can be characterized into two categories: kinetic and kinematic methods [4]. The kinetic methods examine the forces needed for movement. The kinematic methods look at the motion of body segments during locomotion.

One type of sensor used for the kinetic method is the force platform. They are considered the "gold standard" for gait analysis in equine research [4]. The platform measures the ground reaction forces in three dimensions as limbs exert forces during the stance phase. The equipment is typically very precise and accurate. However, the platform's surface area is limited and cannot measure beyond a few strides from an animal. Furthermore, the platform does not lend itself to mass-monitoring of a herd of many cows. There is a development made in the use of force-measuring shoes, but they are not widely available for use and robust enough for practical use [16].

For the kinematic method, optical motion capture systems are highly accurate with an average position error of a few millimeters [4]. They work by putting reflective markers on the animal of study. Several cameras are mounted in the testing area. As the animal moves, the system can track the 3D positions of the markers. However, for a full-body capture of an animal movement, many cameras are needed to give full coverage of the testing area which leads to a significant cost. Similar to the force platform, the method does not scale up economically to monitor many animals.

2.2.3 Inertial Measurement Unit (IMU)

One potential alternative to the optical motion capture system is the usage of inertial measurement units (IMUs). These sensors are attached to the limbs of the subject. As the animal moves, the IMUs report the acceleration and orientation of the sensors. IMUs have been extensively used in human motion studies and their performances have been verified to have comparable performance to optical methods [4]. In recent years, the price of IMUs has dropped due to their wide adoption in the consumer markets. Thus, IMUs make a good candidate for our application.

An IMU is composed of three different sensors: accelerometer, gyroscope, and magnetometer. The accelerometer measures both the acceleration due to Earth's gravity and any additional acceleration due to the animal's motion. However, with just the data from the accelerator alone, the acceleration generated from the animal's motion cannot be decoupled from the Earth's gravitational acceleration. Additional information on the orientation of the sensor must be known and hence the additional usage of the magnetometer and gyroscope.

The gyroscope measures angular velocity, and in theory, it should be enough to provide the orientation measurement needed to decouple the acceleration measurements. However, it suffers bias instabilities in its construction leading to drifts in its measurement. To compensate for this error drift, two reference orientations must be provided. One reference orientation is the Earth's magnetic field which always points North. The magnetometer measures this static magnetic field and its orientation. The second reference orientation is the Earth's gravitation force which always points toward the center of the Earth and can be measured by the accelerometer. These two references provide enough information to resolve the bias drifts from the gyroscope.

To resolve all of these complex measurements into stable and analyzable data, an algorithm called Attitude Heading Reference System (ARHS) is used. Measurements from the accelerometer, magnetometer and gyroscope are combined to provide an estimate of the object's orientation, often using a form of the extended Kalman filter. However, to use a full extended Kalman filter is too computationally intensive to run in real-time with a microcontroller [18]. Thus, onboard many IMUs, algorithms like Madgwick or Maghony algorithm are used instead [7].

2.2.4 Principal Component Analysis (PCA)

Based on the current observation method for lameness score, a lame cow will exhibit an asymmetrical walking rhythm and a bobbing head motion. To fully observe these behaviors, 5 IMUs are used: one at every metacarpus of each limb, and one at the collar. The sensors placed at the metacarpus will allow observation of the asymmetrical walking rhythm. The sensor at the collar will track for head bobbing motion.

Each IMU sensor returns seven data points at every timestamp: quaternion (4 points) and linear acceleration (3 points). With 5 IMUs, at each timestamp, we will observe 35 data points. This high dimensional data set $D \in \mathbb{R}^{N\times 35}$ can be remapped to a smaller dimensional space through Principal Component Analysis. Through this method, redundant dimensions can be removed with minimal effects on the overall integrity of the data. Thus, we can study a smaller dataset without sacrificing signal integrity.

The dataset D can be imagined as a point cloud with each point being in 35 dimensions. This point cloud can be fitted with a 35-dimensional ellipsoid. At the principal axes of this ellipsoid, we can measure the spread or the variance of the dataset along these axes. The axes with minimal spread do not contribute much to describing the dataset and can be eliminated. Thus, we can reduce the dimensions of the dataset, D, while still maintaining the integrity of the data. This is the essential intuition behind Principal Component Analysis [22].

The algotithm can be described as:

1. Calculate the Covariance of the Dataset
   (a) $\Sigma = \mathbb{E}[(\boldsymbol{X} - \mathbb{E}[\boldsymbol{X}])(\boldsymbol{X} - \mathbb{E}[\boldsymbol{X}])^T]$
   (b) The computational complexity of this operation is $\mathbb{O}(NP)$, where P is the amount of parameters and N is the amount of data points
   (c) We can measure the spread of the dataset in direction $\boldsymbol{u}$ with $\boldsymbol{u}^T \Sigma \boldsymbol{u}$. Furthermore, Σ is always a symmetric and positive semi-definite matrix as the variance of data is always positive
2. Calculate the Spectral Decomposition of the Covariance Matrix
   (a) $\Sigma = PAP^T$,
      i. A is a diagonal matrix with its diagonal entries be the eigenvalues, λ_i, of Σ. The eigenvalues are ordered such that $\lambda_1 \geq \lambda_2 \geq ...\lambda_p$.
      ii. The columns of P are the eigenvectors, $\boldsymbol{v_i}$
   (b) The eigenvectors are the principal axes of the fitted ellipsoid onto the data set with its eigenvalue measuring the variance of the data along that axis.
   (c) The worst case computational complexity is $\mathbb{O}(P^3)$. This step is highly computationally intensive and is a roadblock for onboard realtime gait analysis on a microcontroller.
3. Choose a $K < P$ to select for a lower amount of dimensions to represent the data
   (a) $P_K = [\boldsymbol{v_1}, \boldsymbol{v_2}, ...\boldsymbol{v_k}]$, where $\boldsymbol{v_i}$ are the columns of P.
   (b) $P_K \in \mathbb{R}^{P \times K}$
   (c) K is chosen to select for a proportion, α, of the explained variance.

i. $\alpha = \frac{\lambda_1+\lambda_2+...+\lambda_k}{\lambda_1+\lambda_2+...+\lambda_p}$

4. Remap dataset with the new selected dimensions

   (a) $\boldsymbol{Y_i} = P_k^T \boldsymbol{X_i}$

2.2.5 Usage of PCA in Gait Analysis

PCA is well-known for its usage of high dimensionality reduction. However, the method has only been recently used in the analysis of animal movements [10]. The biomechanics of movement is holonomic constraints in nature. Across many mammals like humans, equines, and cattle, the body is composed of skeletal segments connected with ligaments creating hundreds of joints moving together.

To describe the complex motions, thousands of variables are needed to describe the states of each segment. For example, a seven-segments model requires more than 80 variables to describe the linear and rotational velocities and accelerations [10]. However, due to the holonomic constraints of the skeletal segments, the variables are correlated and act in coordination. Thus, data reductions are possible and allow for the identification of patterns and domains. Previous works find kinematic properties of cyclic and arm and leg movements in humans in terms of their phase and frequencies. Furthermore, muscle EMG signal can also be included in the data and reduced through this method [26].

Once a particular motion has been analyzed with PCA, the principal component vectors represented the reorientation of the data points onto the new principal axis. Thus, by examining the principal component vectors, physical interpretations can be made about the modes of each principal component. By looking at the relevance of these modes, different gaits can be differentiated based on their mode weights. In Monaghan et. al works, they examine six dominant components making up 79.15% of the variance of the walking gait of people with multiple sclerosis [20]. The domains are identified to be rhythm, variability, asymmetry, anterior-posterior dynamic stability, and medial-lateral dynamic stability. By looking at the relevance of each of these domains, they were able to differentiate between the gaits of people with sclerosis who has fallen or has not fallen before. Similarly, we can use this technique to differentiate the walking gaits of normal walking and lamed walking cows.

Chapter 3

Design and Experimental of Bovine Sensor Suite

3.1 Design of Wireless Architecture

3.1.1 Functional Requirements

For a typical dairy farm operating under the Fonterra Co-operating Group, the farm has an area of 1500000 m^2 and a herd size of 440 cows [21]. From each individual cow, we would like to acquire health signals.

Mastitis, an inflammation of the udder, is the most common disease negatively affecting the economic output of a dairy farm. The udder inflammatory response leads to a reduction in milk production - on average 11% to 18 % of the gross margin per cow [9]. Furthermore, the disease is contagious and will spread to the rest of the herd. Thus, early detection for treatment and isolation is of utmost importance to a dairy farmer. One particular symptom is an increase in temperature at the udder. With a temperature sensor at the udder, mastitis can be detected [9]

Calving is a dangerous process for both the cow and its calf [8]. Thus, expert human care is recommended, but this is unsustainable to watch for calving on a large farm. There exist a variety of sensing methods for the behavioral and physiological change of cows that can identify this important period of calving [8]. One such behavioral change is in the movement of the cow's tail. As such, an accelerometer can measure such motion. Furthermore, there are variabilities in the behavior of cows that a combination of sensing technologies to increase the accuracy of predicting parturition.

Given all of these parameters, the wireless sensor network must be able to work with a wide variety of sensors each with its own data bandwidth requirement and location placement requirements. The network must be able to support a large number of cows on a farm on the order of thousands. Furthermore, to keep the economic cost low, each node on the sensor network must be inexpensive in upfront cost and maintenance cost. As the size of a free grazing farm can be very large, the range of the network must encompass on the order of a kilometer range in radius.

Figure 3-1: A hypothetical outline of a 1500000 m^2 area dairy farm

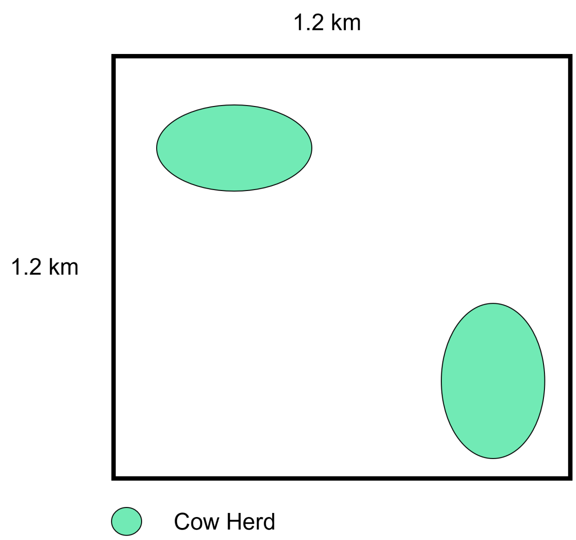

3.1.2 Network Architecture

Unfortunately, there is no existing long-range communication protocol working in the range of 1 kilometer that can simultaneously support high bandwidth data and low energy consumption. To resolve all of the required parameters for this sensor wireless network, a combination of both short-range and long-range communication protocols is selected. For short-range communication, Bluetooth Low Energy is used.

For long-range communication, LoRa is selected.

Within one cow, many sensors are placed at different locations on the body. Instead of connecting each of these sensors together with wires, these sensors communicate with a central node using Bluetooth Low Energy. Not using wires eliminates the risk of the cow rubbing on other objects and ripping the wires apart. Furthermore, Bluetooth Low Energy is capable of transmitting 1 Mb/s of data up to a range of 100 meters while only comsumes 0.66 Watts during transmission. With this capability, high data bandwidth sensors like Inertial Measurement Units or microphones can all relay their data toward a central unit [17].

Figure 3-2: Peripheral sensors transmitting data to a central node at the cow's collar.

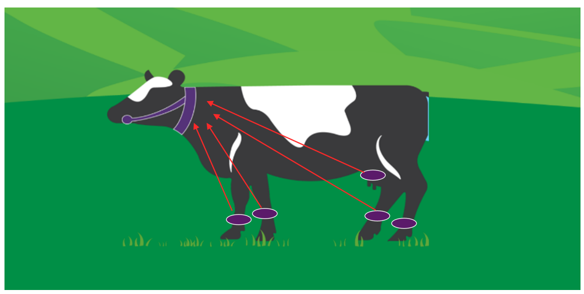

Once the data arrive at the central node, analyses are done onboard. The LoRa protocol can support a 10 kb/s data rate at a distance of 1 kilometer in an open space outdoor environment [15]. During transmission, the protocol only consumes around 0.3 Watts. The protocol can provide tradeoffs and communicate up to a 300-kilometer distance at a 0.6 kb/s data rate. The tradeoff for data rate and distance is logarithmic. After the analyses are done, the central node can communicate with the LoRa gateway to report the current health statistics of that individual cow. With this configuration, all metric analysis must be done onboard the central node, and only the final indicator is sent to the server gateway. The full collected data like the acceleration measurement cannot be sent through the LoRa network.

Another considered alternative to this network configuration is to only used Bluetooth Low Energy. Instead of using the configuration of Central and Peripheral connections, Bluetooth Low Energy supports the creation of a mesh network. Utilizing the fact that cows are herd animals, they will congregate to be near each other even on

Figure 3-3: Each central node on a cow communicates through LoRa to the gateway located somewhere on the farm

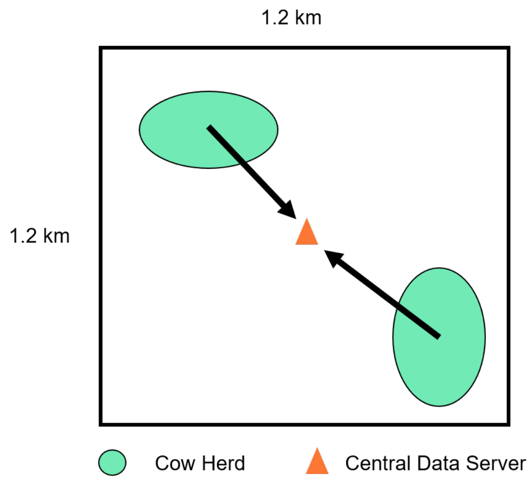

a large farm. Thus, even with short-range communication, data from every cow can be aggregated and collected to a central server. This configuration will allow all the collected data to be sent to a central server through the higher throughput capability of Bluetooth Low Energy. Once the data arrives at a central server, a large processing capability is enabled leading to more advanced and powerful computational analyses being done. However, the trade-off for this configuration is energy saving. In a mesh network, each data packet is repeated and retransmitted many times between each node before the data arrives at a central server (source networking configuration comparison). In turn, the on-time transmission of Bluetooth is higher and consumes significantly more energy consumption.

Through using the combination of LoRa and Bluetooth Low Energy, a star topology network architecture is selected. In this configuration, each data packet is directly traveling in the shortest path to the central data server [5]. As such, the on-time transmission is kept minimal and therefore the lowest energy consumption. As mentioned above, the tradeoff for this configuration requires all data analysis to be onboard each central node. However, the modern processing power of microcontrollers like the Arm Cortex M-4 is sufficiently powerful and has energy efficiency. For example, the nRF52840 System on a Chip that combines both Bluetooth Low Energy technology with an Arm Cortex M-4 processor is clocked to perform at 64 MHz with only 54

μA/MHz of energy consumption. Another risk with this network protocol is packet loss. As each packet is traveling in a direct path to the central server, if the packet is corrupted or failed to deliver along the way, the data is lost. However, this risk can be resolved by having each sensor node have onboard storage space. Data loss can be recovered afterward detection. This is possible as we do not need continuous and live data on the health signals of each cow. A few health reports of each cow per day are sufficient. Thus, data integrity can be accomplished before each central node runs the analyses.

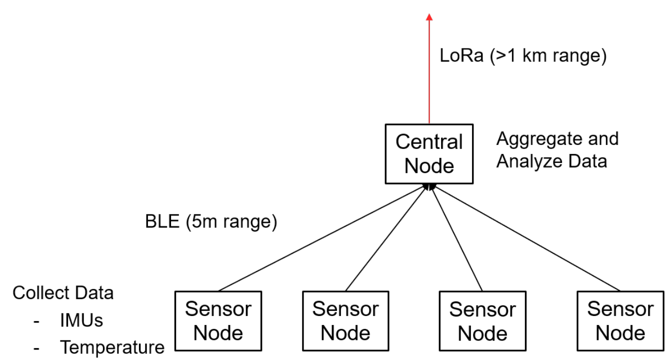

(a) Per cow, there are many sensor nodes and one central node.

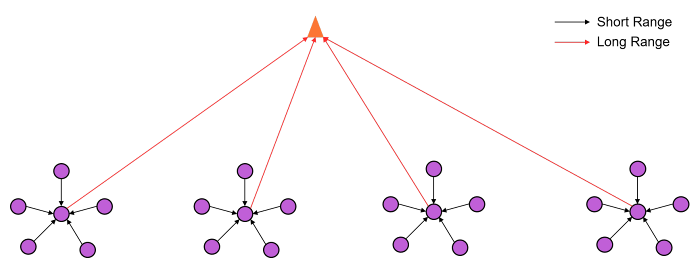

(b) Round circles are nodes. The triange is the gateway.

Figure 3-4: Star topology of the network

3.2 Prototype of Wireless Network

3.2.1 Hardware Selection

The three main components of the network described above are sensor nodes, central nodes, and LoRa Gateway. The sensor nodes are selected to be Arduino Nano 33 BLE

Sense. The main component of this board is a U-Blox NINA-B306 chip. The chip is a stand-alone Bluetooth 5 low energy module with an ARM Cortex-M4 processor. Furthermore, the Arduino Nano 33 BLE Sense comes with an IMU (LSM9DS1), microphone (MP34DT05), light (APDS9960), barometric pressure (LPS22HB), and temperature/humidity (HTS221) sensors. Furthermore, a heart rate sensor (MAX32664) is additionally installed on the Arduino Nano 33 BLE sense board to include a biometric signal. The compact form factor that has Bluetooth Low Energy capability and a plethora of sensors make this board a good choice as a sensor node for this experiment.

Figure 3-5: Sensor node

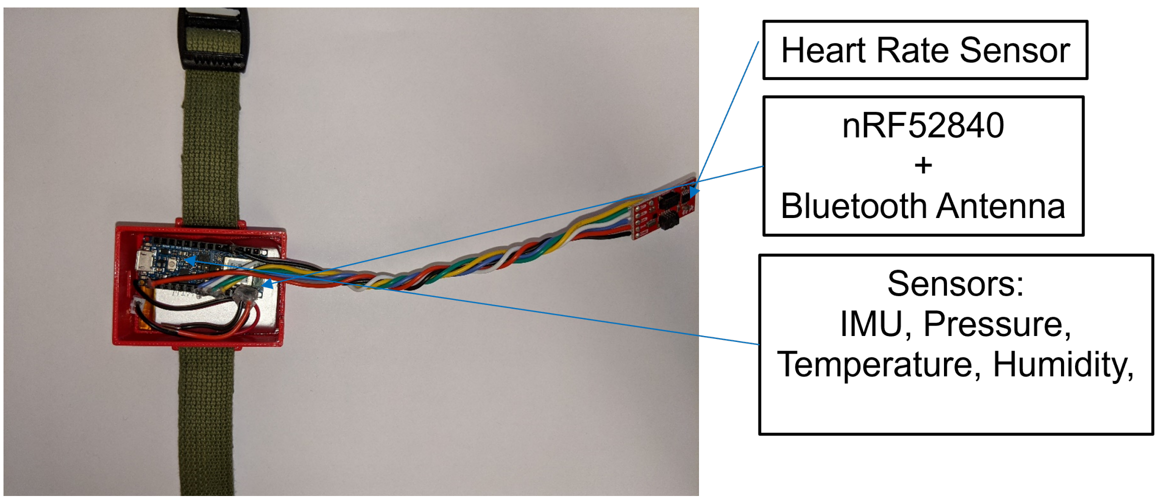

The central node has to support both Bluetooth Low Energy and LoRa communication protocols. RAKWireless RAK4631 module is selected for this task. The chip combines a Nordic nRF52840 microcontroller which has a built-in Bluetooth 5 module with a LoRa transceivers SX126x from Semtech. Furthermore, the module can easily support a GPS connection. The Nordic nRF52840 also has an ARM Cortex-M4 microcontroller which has it sufficiently powerful to do simple data analysis tasks. This makes the chip a convenient choice as the central node.

Finally, the LoRa gateway is selected to be WisGate RAK7249. This gateway is designed for use in outdoor harsh conditions with built-in backup battery power. As a gateway, its task is to receive incoming LoRa packets, decipher the message,

Figure 3-6: Central Node

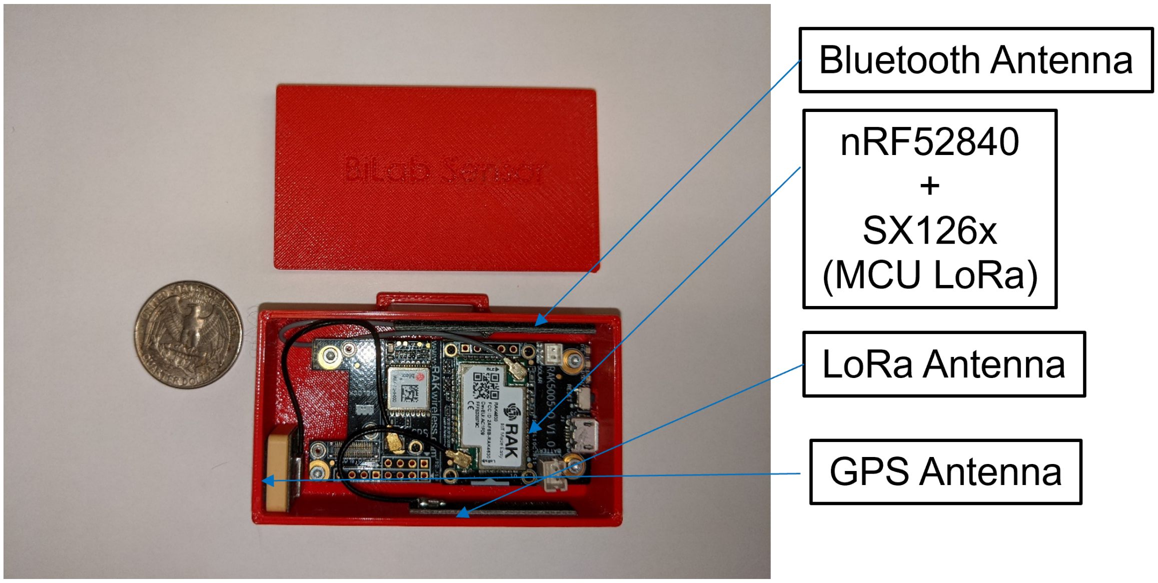

and forward the data toward a server. For our experiment, to receive incoming data, an 8dBi Fiberglass Antenna was designed to work with the 915 MHz frequency to comply with FCC radio regulations. The gateway also has built-in Wi-Fi, ethernet, and cellular connectivity options for connecting to the internet. One important consideration for LoRa communication is that a direct line of sight is required. Thus, it's highly recommended that the gateway be installed up high on top of buildings to be unobstructed.

3.2.2 Network Functionality Test

To test the functionality of this network, each module of the network is tested at the MIT campus. A LoRa gateway is placed on top of Building 1 at MIT facing the Charles River. At this particular location, the LoRa gateway has an unobstructed view of the walking path along the Charles River.

A user straps one sensor node on one wrist and one central node on the other wrist. The sensor node is programmed to act as a peripheral Bluetooth Low Energy module. Following the specifications of the Bluetooth Special Interest Group, the Generic Attribute Profile of the sensor node is the Environmental Sensing Profile [14]. By using a predefined attribute profile, the sensor node is able to be a software

Figure 3-7: LoRa gateway installed on a rooftop

and hardware agnostic device and not specifically tied to only working with this network architecture. The node is set to only update the central node of new data every 10 seconds.

On the other wrist, the central node runs a Central GAP profile to connect to the peripheral sensor node. Specifically, the central node parses the data based on the Bluetooth Environmental Sensing Profile. Furthermore, being a Central Node does not prevent the device from collecting data - equipped on the Central Node is a GPS module. All sensing data are reformatted to LoRa packages which are composed of a series of 8 bits of data. The data sent is represented in the table below. A total of 200 bits is sent per transmission. For this experiment, the central node is set to either send data every 20 seconds while motion is detected or every 1 minute if no motion is detected.

Figure 3-8: LoRa gateway is placed to have unobstructed view of the Charles River's walkway

LoRa Data Package Encoding	
Sensing Data	Number of Bits
Lattitude	32
Longitude	32
Altitude	16
Horizontal Dilution of Position	8
Battery Level	8
Speed	16
Tempurature	16
Humidity	16
Pressure	32
Light Intensity	8
Heart Rate	8
Detected Movement	8

To test if the network can fulfill the functional requirements, the subject is in-

Figure 3-9: Subject wearing a central and a sensor node on each wrist.

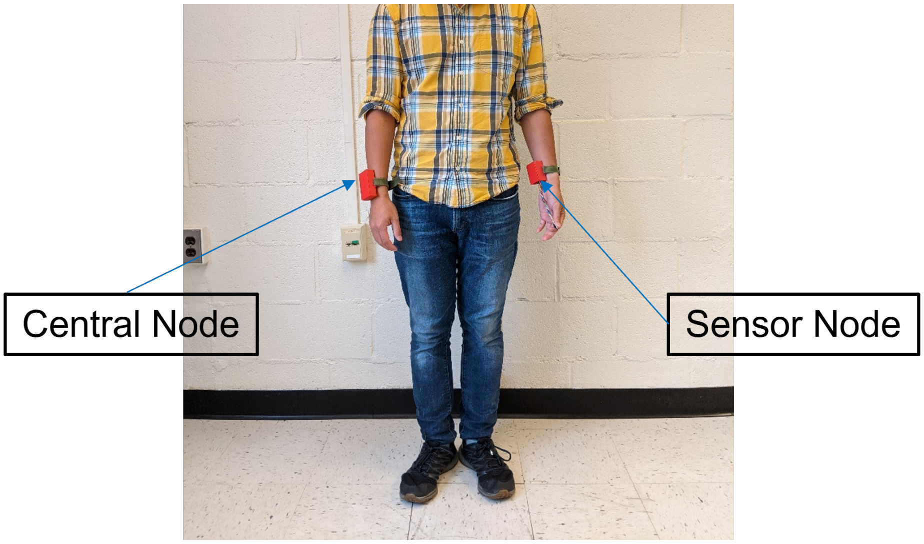

structed to walk along the Charles River to a distance at least 1 Kilometer away from the LoRa gateway. With the constraint of the environment, the subject could only walk 1.5 kilometers away from the gateway before encountering areas with a high amount of line of sight obstructions. Furthermore, as noted on the GPS tracking figure, the signal is lost when there is no direct line of sight when the subject walked underneath bridges. However, due to the attachment of the heart rate sensor to the subject, intermittent heart rate data is collected during the walking motion. Thus, a portion of the collected heart rate is measured as zero when the heart rate sensor (MAX32664) reported the measurement with low confidence.

With this experimental setup, power consumption measurement is made for the central node and sensor node. Based on the measurement, for a sensor node to continuously measure and transmit data for 15 minutes a day, the sensor can run for 178 days or almost 6 months on a Lithium-Ion coin cell. This is also a very conservative estimate as the sensor does not continuously transmit data through Bluetooth. It will only communicate with the central node when there is newly available data. As for the central node, the maximum power consumption is when both Bluetooth and LoRa transmission is operating at the same time at 39.37 mA. One advantage of the central node is that the device can be placed anywhere on the body and not limited to a specific location to collect some health data. The central node can be placed

Figure 3-10: GPS tracking of the subject during their walk.

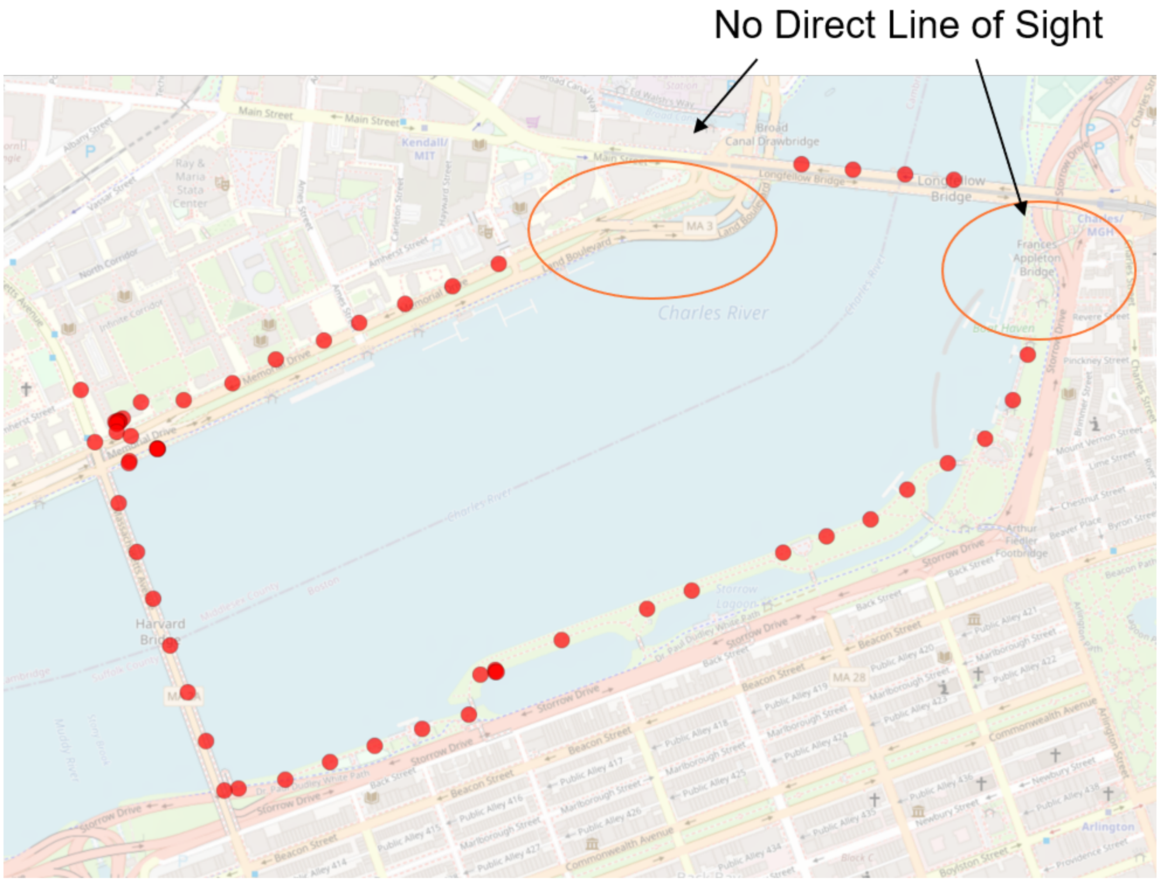

strategically at the cow's collar to be exposed to sunlight. A small solar panel the size of 89mm x 113mm can generate a peak current of 180 mA. In combination, this means the central node can operate indefinitely.

Sensor Node Power Consumption	
State	Average Current Consumption
Idling	11.81 μA
Sensors Online	8.95 mA
Bluetooth Online	18.30 mA
Bluetooth Transmitting	22.46 mA

Figure 3-11: Heart rate measurement of the subject during their walk.

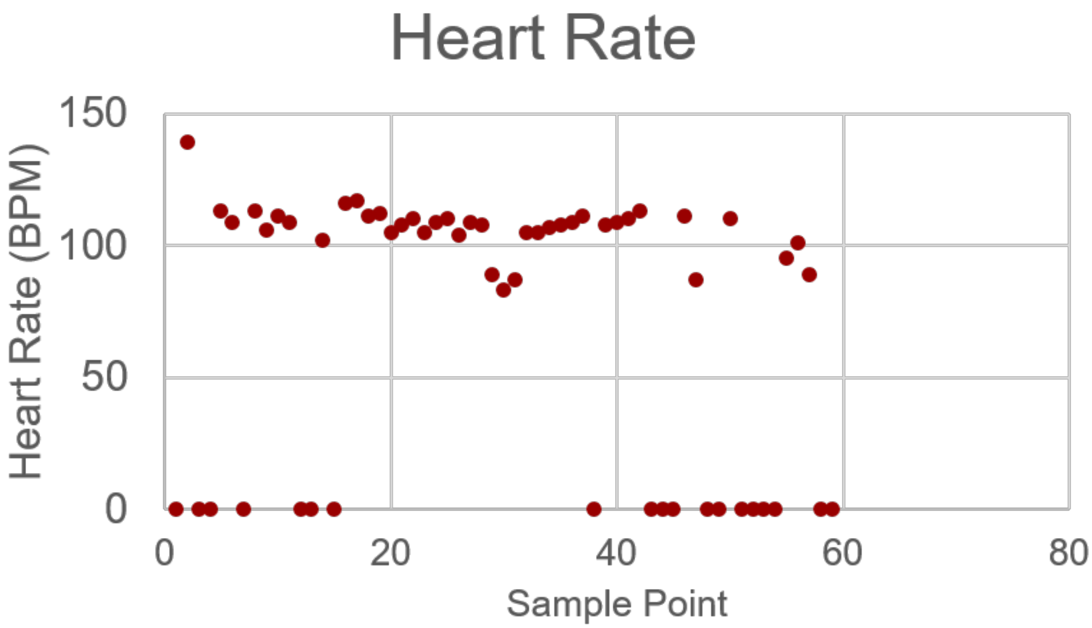

Central Node Power Consumption	
State	Average Current Consumption
Idling	12.81 μA
Bluetooth and LoRa Transmitting	39.37 mA

From these preliminary results, the proposed architecture can sufficiently fulfill all the functional requirements for the health monitoring of cows on a farm. The design is flexible enough to work with many types of sensors. Additionally, the wireless nature of the sensors allows them to be mounted at any location on the cow to properly capture the desired health signal. With the constraint of the environment, we can only test the long-range communication of the sensors up to 1.5 kilometers, but they should be capable to work at a much longer range. However, even at 1.5 kilometers, the LoRa protocol should be sufficient to work with most fairy farms. The power consumption from these two low-energy communication protocols is sufficient such that farmers only have to spend much time swapping batteries on the sensors every 6 months.

3.3 Proposed Experiment Design for Gait Analysis on Cows

While the network is designed to work as an overall health monitoring system, in this work, we focus our effort on only looking at lameness in cows. At this time, detection is based on subjective locomotion scoring to recognize changes in gait patterns. By using inertial measurement units, we can develop a more objective and reliable method for the early detection of lameness. Furthermore, lameness is a condition caused by many different diseases and injuries. Identification of the underlying cause of the lameness is valuable for treatment and overall farm management. The more accurate and systematic measurement may provide a correlation with the underlying causes of the lameness. Additionally, the computational and data bandwidth requirement of this problem is most challenging. If this problem can be successfully solved, the other health monitoring tasks should also be solved

However, due to the extensive regulatory requirements for animal research, we, unfortunately, could not run the following proposed experiments to collect walking gait data on cows.

3.3.1 Sensors

Five inertial measurement units (herein referred to as MIT IMUs) will be attached to each of the 10 cows used in this study. One MIT IMU will be affixed to a collar worn by the cow while one each of the remaining four will be attached to the lower aspect of each of the cows' limbs – more specifically the lower aspect of the metacarpus/metatarsus (mid-hand/midfoot bones) respectively. To access the performance of the MIT IMUs, two cows will also be outfitted with 5 commercially available IMUs (INERTIA Technology ProMove-mini IMUs – hereafter referred to as PMM IMUs). The PMM IMUs have been extensively tested for performance in use with other gait analysis experiments [4][25]. They will also be used to validate the performance of the self-produced MIT IMUs. Both IMUs are set to collect orientation data and body forces acceleration on 3 axes at 200 Hz.

Figure 3-12: MIT IMU sensor compared to a cow metacarpus

3.3.2 Experimental Design

Field Study Site

This study will be carried out at Fairvue Farms in Woodstock, CT. Fairvue is a client of the Tufts Veterinary Field Service of the Cummings School of Veterinary Medicine at Tufts University. Prior to beginning any study, the client/owner will need to sign a TUFT's IACUC Owner Consent Form for application of the IMUs discussed above.

Acclimation

A total of 10 cows aged 4-5 years with similar body size and parity, if possible, will be used in this study. Using locomotion scoring, five of the cows will be identified as having a normal gait (non-lame) and 5 will be identified as being mid to moderately lame (a score of 2 -mildly lame with back slightly arched when walking or 3 – moderately lame with arched back when both standing and walking and short strides, head down respectively)[24]. Visual assessment using subjective locomotion scoring will be done by a licensed veterinarian from the Cummings School of Veterinary Medicine at Tufts University who practiced in the field.

All animals will be acclimated, if required, to wearing a collar to which one of the 5 MIT IMUs (25 g; 75 x 25 x 25 mm) will be attached. Of the 4 remaining MIT IMUs, one each will be strapped to the lower part of each of the cow's limbs. Two of the cows designated as non-lame will also be outfitted with 5 PMM IMUs (20 g; 51 x 46 x 15 mm), the IMUs being placed on the cow in proximity to the MIT IMUs. Each system will be attached to the lower limbs using a strap as done for the pedometers currently worn by the cows. To reduce stress, the devices will be strapped to and removed from the cows by a member(s) of the farm who routinely handles the animals.

Pilot studies to assess normal gait

Currently, the cows to be used in this study are housed in a free-stall barn. Three times a day, they actively walk from the barn to the milking area 100 m distant wherein they are milked, and then walk back to the barn. This is a well acclimated, repetitive procedure requiring a total time of approximately 1 hour. We plan to monitor 5 cows exhibiting normal gait (no lameness) on their way to and from the milking parlor on two separate occasions. Of the 5 animals, 3 will wear MIT IMUs and 2 will wear MIT IMUs and PPM IMUs as discussed above. The outcome of this study should 1) provide a baseline for the kind of data we expect to collect from non-lame cows and 2) provide some measure of the replicability of the data collected within and between experiments and IMUs. Ideally, this would be done in a single day with the 1st and 2nd, 2nd and 3rd, or 1st and 3rd milking periods, each period representing a single pilot study.

Because we cannot walk alongside the cows, they will be observed at a distance with data collected saved on board from both the MIT IMUs and the PMM IMUs. The IMUs will be synchronized to begin collecting data at the same time via a remote signal from the individual conducting the study. Remote signaling will also be used to end data collection. At this time, all IMUs will be removed from those animals tested at the end of the test day to permit the data collected to be downloaded for analysis. With the pilot studies, the goal is to verify the robustness of the MIT IMUs in which we can acquire replicable and analyzable data from the two milking periods.

Figure 3-13: Schematic of Cows Movement During Milking

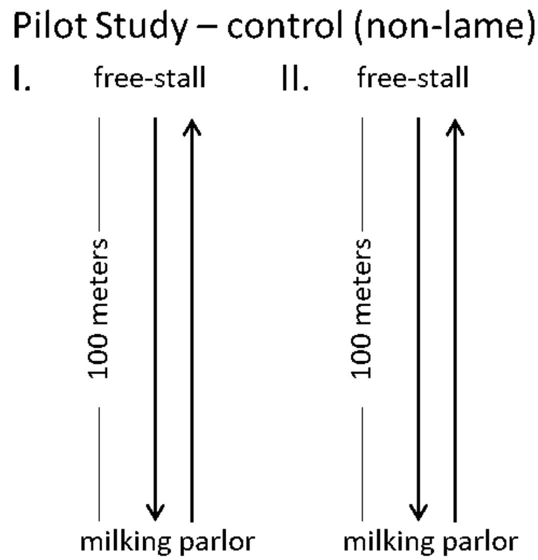

Gait study to identify lameness

Following successful pilot studies, a follow-up gait study is run. The gait study will use 10 animals, 5 lame and 5 showing no signs of lameness, to evaluate the ability of our hardware/software to differentiate lame from non-lame animals. All the animals will be outfitted with MIT IMUs placed. However, two of the lamed cows will also be outfitted with the PMM IMUs. The intent is again to provide a set of validation data from an established commercial product.

Using the walking gait data from this study, we can begin to study how to best differentiate the abnormal and normal cow walking gaits. Additionally, we could use the results to identify the best sensor placement locations. While the 5 locations selected to place the IMUs are based on traditional observation done by veterinarians, they serve to observe the asymmetric walking motions between the fore and hind legs and the vertical bobbing motion of the head. However, the data could show that sufficient data can be observed from a smaller subset of the 5 IMUs. Thus, this gait analysis problem can be solved at a lower cost.

3.4 Experiment on Gait Analysis of Abnormal Human Walking Gait

Without permission to collect data on walking cows, we perform another experiment to showcase the capability of differentiating between normal and abnormal gait. For this study, the author uses the sensor nodes to collect data on his own walking gaits. The analysis method performs here highlights the need to use dimensionality reduction on multiple IMUs data and the need to use multiple IMU to collect walking gaits. In Tijssen's work, they looked at the full spectrum of available data collected from 11 IMUs mounted on a walking cow, the analysis however does not take into account the highly correlated nature of walking gaits in which joints are under a holonomic constraint [25]. This led to a highly tedious feature extraction process to understand the parameters of cow walking gaits. In Haladjian's work, they only collected data from 1 IMU mounted at a hind leg [13]. This led to an easier feature extraction process, but this method does not take into account the symmetrical or asymmetrical nature of multiple limbs moving. With our experiment, we seek to showcase the possibility to use multiple IMUs in a data-efficient manner with dimensionality reduction through the use of Principal Component Analysis and the need to look at the asymmetry of different limbs movement.

3.4.1 Experimental Design

The IMUs selected for this experiment are the INERTIA Technology ProMove-mini IMUs. A person wears two IMUs each attached with velcro straps at their inner ankles. The person is instructed to walk in a straight line for 10 meters under three different footwear conditions. To represent a normal walking gait, the person walks while only wearing socks. To represent an abnormal walking gait, the person walks with only one shoe - either an only right shoe or a left shoe. For each of the three footwear conditions, 24 trials are collected. For each trial, the person is instructed to always start the walk with their right foot. The IMUs collect orientation data and linear acceleration data at 200 Hz.

Figure 3-14: Schematic of Human Walking Experiment

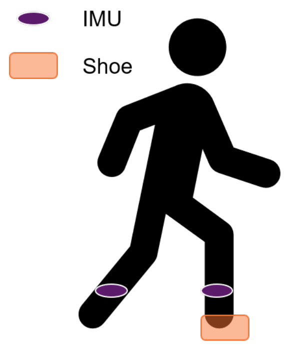

3.4.2 Data Analysis

Preprocessing

For each trial, the data from the first walking step and last walking step are excluded. We want to look at the steady-state walking conditions and not at the acceleration condition from starting to walk and ending the walk of each trial. For each trial, the first step is taken with the right foot. Thus, to exclude this step, we look at the accelerating profile of the left foot. We only keep the data at the time stamp at the first peak acceleration to the second to last peak acceleration. The peak accelerations correspond to the moment the left foot hit the ground. Thus, by looking for this timestamp, we eliminate the data from the time of the right foot and left foot finishing their first full stride. Next, an individual walking stride is exacted using a peak detection method. Every stride is defined as 250 data points (1.25 seconds of data) starting from the peak acceleration point on the left foot X-axis acceleration.

The IMUs measure the net acceleration on the device and thus measure both the body acceleration and gravitational acceleration. In this work, we are only interested in looking at the body acceleration caused by the movement of the foot and not

Figure 3-15: Excluding the first and last step of each walking trial. Only the data between the dash lines are kept.

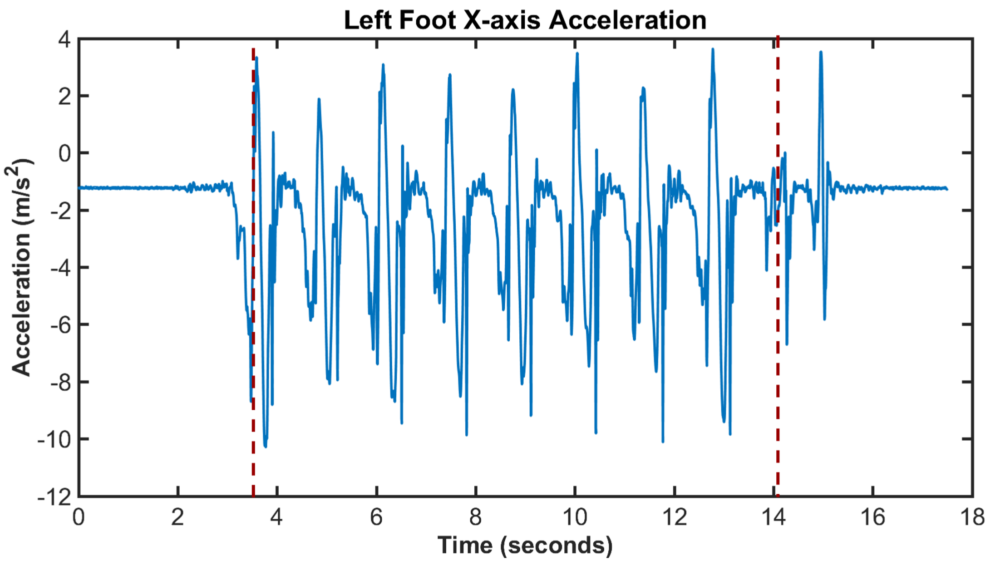

the acceleration caused by gravity. Using the quaternion orientation data, we can remove the gravitational bias. Furthermore, the acceleration is linearly rescaled to be a proportion of the gravitational constant. This scaling allows for a comparable range between acceleration and quaternion value.

$$\boldsymbol{a_{body}} = \boldsymbol{R}^T(\dot{\boldsymbol{v}} - \boldsymbol{g_0}).$$

PCA: Dimensional Reduction

For each IMU, the data collected is the orientation data in the form of quaternion (q_1, q_2, q_3, q_4) and linear acceleration (a_x, a_y, a_z). In total, the data set $D \in \mathbb{R}^{N \times 14}$. As 14-dimensional data, it's time-consuming to inspect for features in each dimension. The computational complexity of such a search would be $\mathbb{O}(PN)$, where P is the number of dimensions (14 in this case). However, to look at the cross-correlation data between each dimension, the computational complexity would be $\mathbb{O}(P^2N)$. This comes from the fact that to cross-correlate between any 2 of P dimensions would be $\binom{P}{2} = P^2/2 - P/2$. To reduce the burden of feature search, a dimensional reduction can be done with Principal Component Analysis (PCA).

Figure 3-16: One Stride of the sock wearing condition

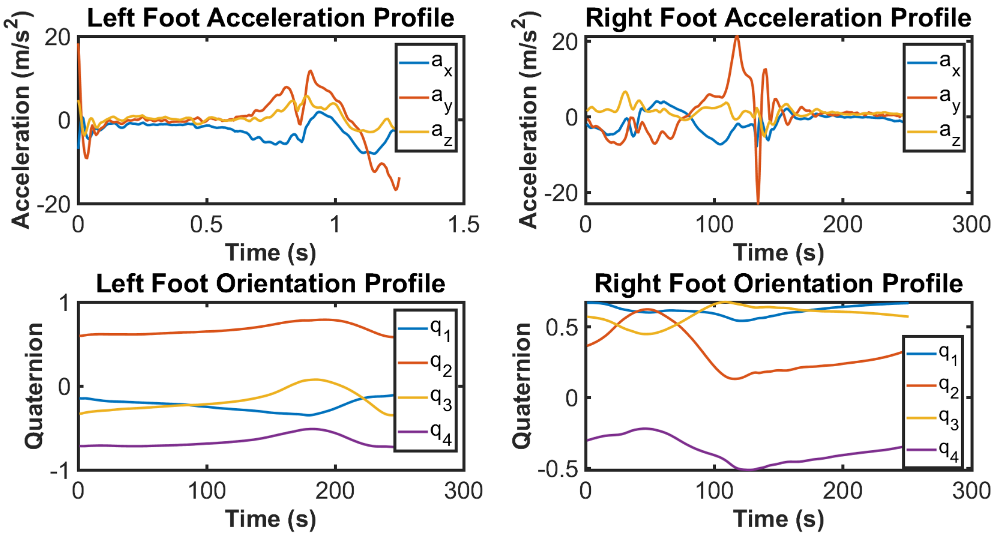

Looking at the eigenvalues of the principal components, we can see that for all three walking conditions only the top 4 principal components are needed to explain the majority of the variance in the data. For socks-wearing condition, the top 4 principal components explain 93.03% of the variance; for left shoe wearing, 92.05%; and for right shoe wearing, 92.72%. Thus, we can safely represent the whole data set with just four dimensions.

PCA orients the data set in a way that will maximize variance per component direction. The method does not try to preserve any physical meaning during the reorientation. Even so, we can still look at each of the principal components to make an interpretation of its physical meaning. Looking at Figure 3-18, we can see how the weights of each measurement for each component direction. Component 1 emphasizes the motion of the right foot acceleration - the biggest weight is the right foot y-axis acceleration. Component 2 emphasizes the motion of the left foot acceleration - the biggest weights are on the accelerations of the left foot. Component 3 emphasizes the orientation of the left foot while component 3 looks at the orientation of the right foot. This phenomenon of pair-wise combinations of left and right foot acceleration matching and left and right foot orientation matching, agrees with other experimental results in using PCA to analyze animal location [10]. We use the principal components

Figure 3-17: The proportion of the explained variance by each principal component

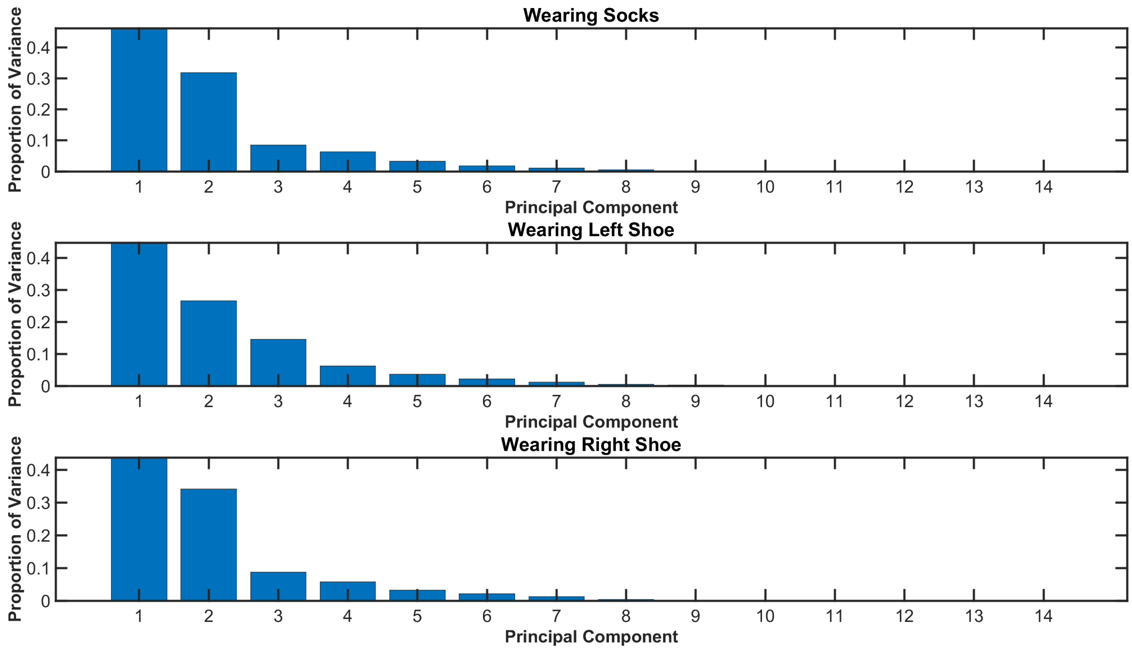

of the socks-wearing condition as the baseline to compare our different gaits. To differentiate the gaits, we observe the data "spatially" and on the time axis.

Data 'Spatial' Observation

After we have reduced the dimension of the data to 4, we can create a point cloud from all of the data points. However, since the data is in 4 dimensions, the presentation of the data is a challenge. In Figure 3-19, we plot the data in a series of 2D scatter plots between each of the respective 4 dimensions. For each type of walking gait, we can see a different point cloud shape.

In particular, between Axis 1 and Axis 3, we can see a linear shift in the shape of the three point clouds. Following our interpretation of the principal axis, the comparison between axis 1 and axis 3 is between the right foot acceleration and left foot orientation. This shift in point cloud indicates an asymmetry changes between the left and right foot during the walk-in abnormal gaits.

Furthermore, we can see that the point cloud for the left shoe-wearing condition

Figure 3-18: The weighted scores of each parameter in in the principal axes

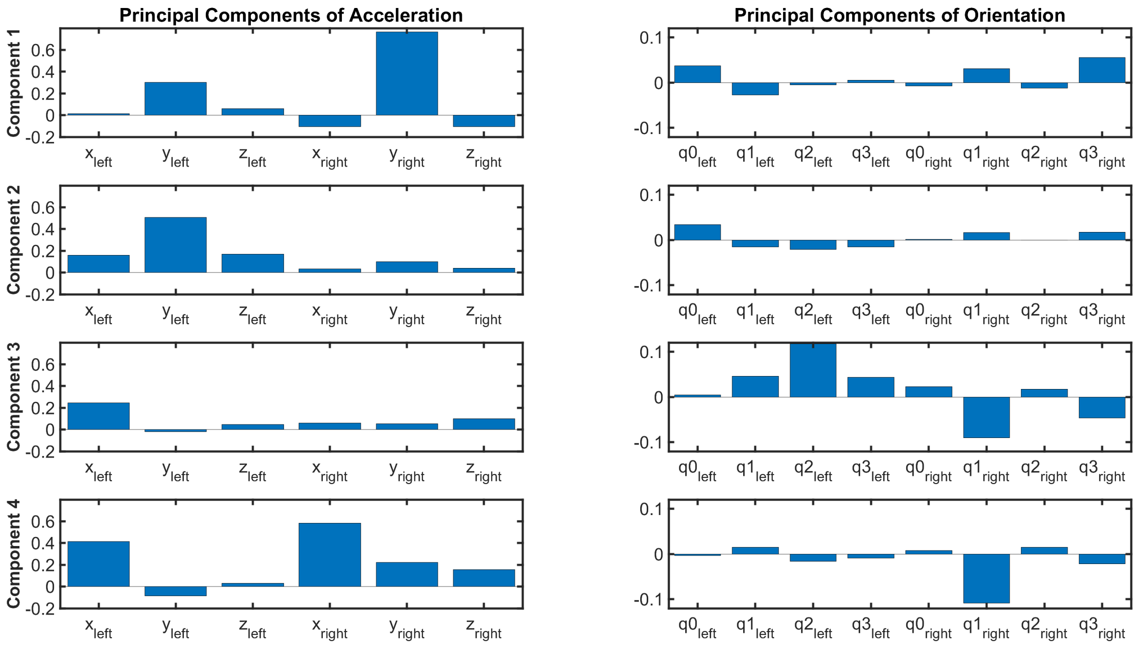

is more differentiable to the baseline than the right shoe-wearing condition. For all the axis comparisons, the left wearing shoe point cloud experiences a bigger linear shift than the right wearing shoe. This indicates that just wearing a left shoe created a more abnormal walking gait for this test subject.

Data 'Time' Observations

A powerful method to observe the time component of the data is through the use of cross-correlation. By comparing the cross-correlation between each axis, we can find asymmetrical features in the data. In Figure 3-20, we can observe the same trend in the "spatial observations". The cross-correlation between axis 2 and axis 3 shows diverging results between the three footwear conditions (at zero shift, socks = 0.369; right = 0.684; left = -0.534). A similar trend can be seen on axis 1 & axis 3, axis 1 & axis 4. The data also indicates that the left shoe-wearing condition generates a more abnormal walking gait. As seen in the cross-correlation between axis 2 & axis 4, the cross-correlation for socks and right footwear conditions are similar compared to left

Figure 3-19: Point cloud data between different axes

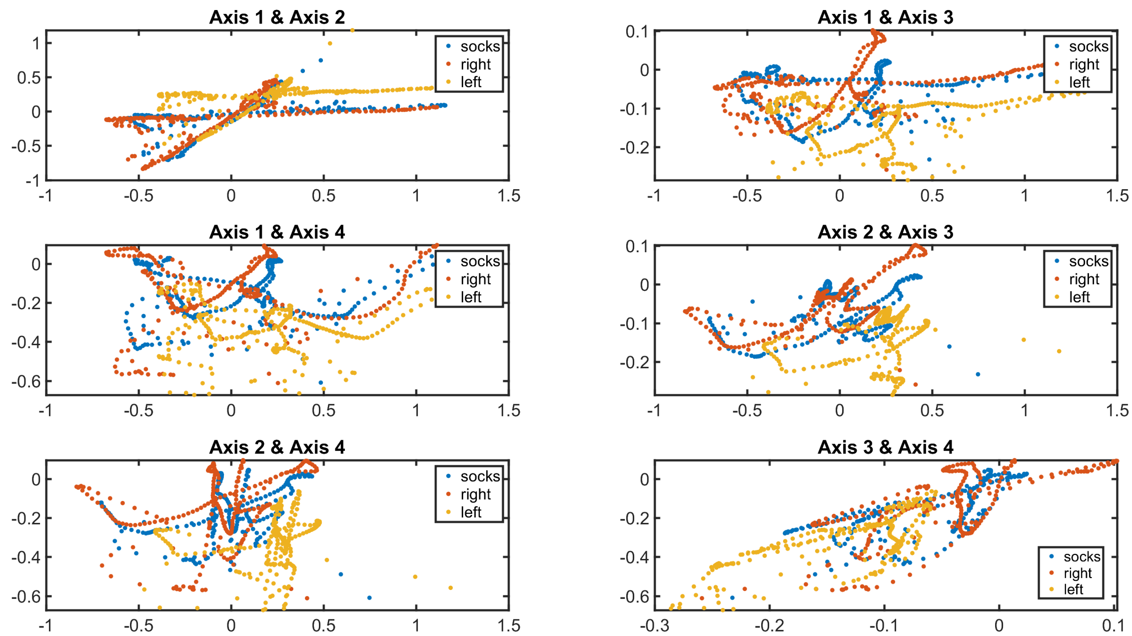

footwear condition (at zero shift, socks = 0.31, right = 0.39, left = -0.59).

Extension for Automated Gait Analysis for Cows

The results from this experiment are promising. Using IMUs, we have shown that normal and abnormal gaits can be differentiated. Furthermore, we could identify the two different abnormal gaits (left shoe vs right shoe). Should this work be transferrable to cows' walking gait, we could identify abnormal walking gaits as the cows deviate from a normal baseline. Furthermore, we could possibly tell the type of injuries and diseases associated with the detected abnormality. However, further work must be done to allow for the automated prediction of lameness in walking cows.

One difficulty with this method is the spectral decomposition step within PCA. The computational complexity of this step is $\mathbb{O}(P^3)$. Thus, with more IMUs mounted on the cow, the computation task is exponentially more challenging. One possible method to reduce this burden is the use of an iterative method for the eigenvalue problem. Working with the assumption that all cows have similar walking gaits, we

Figure 3-20: Cross correlation data between different axes

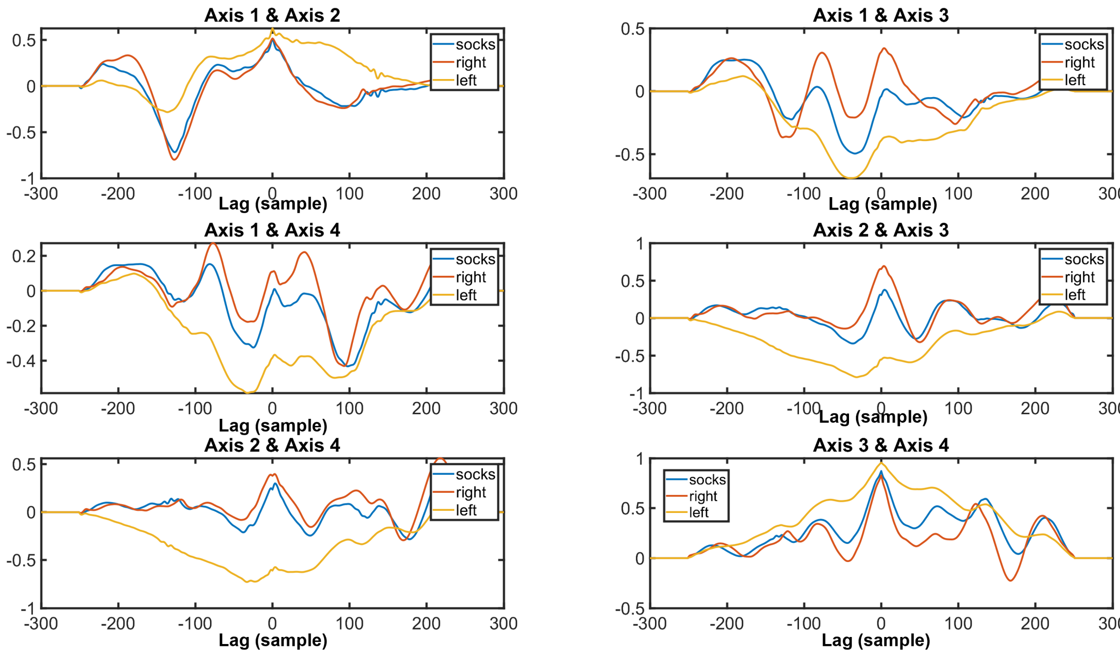

can provide the algorithm with good initial guesses for the eigenvectors. Furthermore, the iterative method can be used to only find a specific number of highest variance eigenvectors, so we would not have to perform an exhaustive search for all the principal axes.

Another challenge is the automated feature extractions and classification. After the dimensional reduction, we must be able to extract characteristic parameters from the data set to feed a classification model. One model we could train is the generalized linear regression. Given a set of feature parameters, we can compute a probability distribution to predict whether a particular gait is abnormal or not. The challenge of classification is that we must train the model using a large repertoire of collected data which cannot be done on the microcontroller on the cow. The onboard computing system must have a trained classification model. With variation in walking gait between cows, the risk is that the classification model would have an incorrect baseline to predict lameness. Further work must be done to explore this problem once data from walking cows are collected.

Bibliography

[1] Ferran Adelantado, Xavier Vilajosana, Pere Tuset-Peiro, Borja Martinez, Joan Melia, and Thomas Watteyne. Understanding the limits of LoRaWAN. *IEEE Communications Magazine*, 55(9):34–40, 2017. arXiv: 1607.08011.

[2] João Sucena Afonso, Mieghan Bruce, Patrick Keating, Didier Raboisson, Helen Clough, George Oikonomou, and Jonathan Rushton. Profiling Detection and Classification of Lameness Methods in British Dairy Cattle Research: A Systematic Review and Meta-Analysis. *Frontiers in Veterinary Science*, 7, 2020.

[3] Simon Archer, Nicholas Bell, and Jon Huxley. Lameness in UK dairy cows: A review of the current status. *in Practice*, 32:492–504, December 2010.

[4] Stephan Bosch, Filipe Serra Bragança, Mihai Marin-Perianu, Raluca Marin-Perianu, Berend Jan Van der Zwaag, John Voskamp, Willem Back, René Van Weeren, and Paul Havinga. EquiMoves: A Wireless Networked Inertial Measurement System for Objective Examination of Horse Gait. *Sensors*, 18(3):850, March 2018. Number: 3 Publisher: Multidisciplinary Digital Publishing Institute.

[5] Stefan Bouckaert, Eli De Poorter, Pieter De Mil, Ingrid Moerman, and Piet Demeester. Interconnecting Wireless Sensor and Wireless Mesh Networks: Challenges and Strategies. In *GLOBECOM 2009 - 2009 IEEE Global Telecommunications Conference*, pages 1–7, November 2009. ISSN: 1930-529X.

[6] E Bäumker, A Miguel Garcia, and P Woias. Minimizing power consumption of LoRa ® and LoRaWAN for low-power wireless sensor nodes. *Journal of Physics: Conference Series*, 1407(1):012092, November 2019.

[7] A. Cavallo, A. Cirillo, P. Cirillo, G. De Maria, P. Falco, C. Natale, and S. Pirozzi. Experimental Comparison of Sensor Fusion Algorithms for Attitude Estimation. *IFAC Proceedings Volumes*, 47(3):7585–7591, January 2014.

[8] Anita Z Chang, David L Swain, and Mark G Trotter. Towards sensor-based calving detection in the rangelands: a systematic review of credible behavioral and physiological indicators. *Translational Animal Science*, 4(3):txaa155, August 2020.

[9] Wei Nee Cheng and Sung Gu Han. Bovine mastitis: risk factors, therapeutic strategies, and alternative treatments — A review. *Asian-Australasian Journal of Animal Sciences*, 33(11):1699–1713, November 2020.

[10] Andreas Daffertshofer, Claudine J. C. Lamoth, Onno G. Meijer, and Peter J. Beek. PCA in studying coordination and variability: a tutorial. *Clinical Biomechanics (Bristol, Avon)*, 19(4):415–428, May 2004.

[11] Carles Gomez, Joaquim Oller, and Josep Paradells. Overview and Evaluation of Bluetooth Low Energy: An Emerging Low-Power Wireless Technology. *Sensors*, 12(9):11734–11753, August 2012.

[12] Bluetooth Special Interest Group Group. Bluetooth Core Specification, July 2021.

[13] Juan Haladjian, Johannes Haug, Stefan Nüske, and Bernd Bruegge. A Wearable Sensor System for Lameness Detection in Dairy Cattle. *Multimodal Technologies and Interaction*, 2(2):27, June 2018. Number: 2 Publisher: Multidisciplinary Digital Publishing Institute.

[14] Donna Hill. ENVIRONMENTAL SENSING PROFILE. page 31.

[15] Thomas Janssen, Noori BniLam, Michiel Aernouts, Rafael Berkvens, and Maarten Weyn. LoRa 2.4 GHz Communication Link and Range. *Sensors (Basel, Switzerland)*, 20(16):4366, August 2020.

[16] M. Kai, O. Aoki, A. Hiraga, H. Oki, and M. Tokuriki. Use of an instrument sandwiched between the hoof and shoe to measure vertical ground reaction forces and three-dimensional acceleration at the walk, trot, and canter in horses. *American Journal of Veterinary Research*, 61(8):979–985, August 2000.

[17] Elke Mackensen, Matthias Lai, and Thomas M. Wendt. Bluetooth Low Energy (BLE) based wireless sensors. In *2012 IEEE SENSORS*, pages 1–4, October 2012. ISSN: 1930-0395.

[18] Sebastian Madgwick. An efficient orientation filter for inertial and inertial / magnetic sensor arrays. *undefined*, 2010.

[19] David C. Van Metre, John R. Wenz, and Franklyn B. Garry. Lameness in Cattle:. *American Association of Bovine Practitioners Conference Proceedings*, pages 40–43, September 2005.

[20] Andrew S. Monaghan, Jessie M. Huisinga, and Daniel S. Peterson. The application of principal component analysis to characterize gait and its association with falls in multiple sclerosis. *Scientific Reports*, 11(1):12811, December 2021.

[21] NZIER. New Zealand Dairy Statistics, November 2017.

[22] Karl Pearson. LIII. On lines and planes of closest fit to systems of points in space. *The London, Edinburgh, and Dublin Philosophical Magazine and Journal of Science*, 2(11):559–572, November 1901. Publisher: Taylor & Francis _eprint: https://doi.org/10.1080/14786440109462720.

[23] Jan K. Shearer, Sarel R. Van Amstel, and Bruce W. Brodersen. Clinical diagnosis of foot and leg lameness in cattle. *The Veterinary Clinics of North America. Food Animal Practice*, 28(3):535–556, November 2012.

[24] P. T. Thomsen, L. Munksgaard, and F. A. Tøgersen. Evaluation of a Lameness Scoring System for Dairy Cows. *Journal of Dairy Science*, 91(1):119–126, January 2008.

[25] M. Tijssen, F. M. Serra Braganca, K. Ask, M. Rhodin, P. H. Andersen, E. Telezhenko, C. Bergsten, M. Nielen, and E. Hernlund. Kinematic gait characteristics of straight line walk in clinically sound dairy cows. *PLOS ONE*, 16(7):e0253479, July 2021. Publisher: Public Library of Science.

[26] D. A. Winter and H. J. Yack. EMG profiles during normal human walking: stride-to-stride and inter-subject variability. *Electroencephalography and Clinical Neurophysiology*, 67(5):402–411, November 1987.

Bibliography

[1] Ferran Adelantado, Xavier Vilajosana, Pere Tuset-Peiro, Borja Martinez, Joan Melia, and Thomas Watteyne. Understanding the limits of LoRaWAN. *IEEE Communications Magazine*, 55(9):34–40, 2017. arXiv: 1607.08011.

[2] João Sucena Afonso, Mieghan Bruce, Patrick Keating, Didier Raboisson, Helen Clough, George Oikonomou, and Jonathan Rushton. Profiling Detection and Classification of Lameness Methods in British Dairy Cattle Research: A Systematic Review and Meta-Analysis. *Frontiers in Veterinary Science*, 7, 2020.

[3] Simon Archer, Nicholas Bell, and Jon Huxley. Lameness in UK dairy cows: A review of the current status. *in Practice*, 32:492–504, December 2010.

[4] Stephan Bosch, Filipe Serra Bragança, Mihai Marin-Perianu, Raluca Marin-Perianu, Berend Jan Van der Zwaag, John Voskamp, Willem Back, René Van Weeren, and Paul Havinga. EquiMoves: A Wireless Networked Inertial Measurement System for Objective Examination of Horse Gait. *Sensors*, 18(3):850, March 2018. Number: 3 Publisher: Multidisciplinary Digital Publishing Institute.

[5] Stefan Bouckaert, Eli De Poorter, Pieter De Mil, Ingrid Moerman, and Piet Demeester. Interconnecting Wireless Sensor and Wireless Mesh Networks: Challenges and Strategies. In *GLOBECOM 2009 - 2009 IEEE Global Telecommunications Conference*, pages 1–7, November 2009. ISSN: 1930-529X.

[6] E Bäumker, A Miguel Garcia, and P Woias. Minimizing power consumption of LoRa ® and LoRaWAN for low-power wireless sensor nodes. *Journal of Physics: Conference Series*, 1407(1):012092, November 2019.

[7] A. Cavallo, A. Cirillo, P. Cirillo, G. De Maria, P. Falco, C. Natale, and S. Pirozzi. Experimental Comparison of Sensor Fusion Algorithms for Attitude Estimation. *IFAC Proceedings Volumes*, 47(3):7585–7591, January 2014.

[8] Anita Z Chang, David L Swain, and Mark G Trotter. Towards sensor-based calving detection in the rangelands: a systematic review of credible behavioral and physiological indicators. *Translational Animal Science*, 4(3):txaa155, August 2020.

[9] Wei Nee Cheng and Sung Gu Han. Bovine mastitis: risk factors, therapeutic strategies, and alternative treatments — A review. *Asian-Australasian Journal of Animal Sciences*, 33(11):1699–1713, November 2020.

[10] Andreas Daffertshofer, Claudine J. C. Lamoth, Onno G. Meijer, and Peter J. Beek. PCA in studying coordination and variability: a tutorial. *Clinical Biomechanics (Bristol, Avon)*, 19(4):415–428, May 2004.

[11] Carles Gomez, Joaquim Oller, and Josep Paradells. Overview and Evaluation of Bluetooth Low Energy: An Emerging Low-Power Wireless Technology. *Sensors*, 12(9):11734–11753, August 2012.

[12] Bluetooth Special Interest Group Group. Bluetooth Core Specification, July 2021.

[13] Juan Haladjian, Johannes Haug, Stefan Nüske, and Bernd Bruegge. A Wearable Sensor System for Lameness Detection in Dairy Cattle. *Multimodal Technologies and Interaction*, 2(2):27, June 2018. Number: 2 Publisher: Multidisciplinary Digital Publishing Institute.

[14] Donna Hill. ENVIRONMENTAL SENSING PROFILE. page 31.

[15] Thomas Janssen, Noori BniLam, Michiel Aernouts, Rafael Berkvens, and Maarten Weyn. LoRa 2.4 GHz Communication Link and Range. *Sensors (Basel, Switzerland)*, 20(16):4366, August 2020.

[16] M. Kai, O. Aoki, A. Hiraga, H. Oki, and M. Tokuriki. Use of an instrument sandwiched between the hoof and shoe to measure vertical ground reaction forces and three-dimensional acceleration at the walk, trot, and canter in horses. *American Journal of Veterinary Research*, 61(8):979–985, August 2000.

[17] Elke Mackensen, Matthias Lai, and Thomas M. Wendt. Bluetooth Low Energy (BLE) based wireless sensors. In *2012 IEEE SENSORS*, pages 1–4, October 2012. ISSN: 1930-0395.

[18] Sebastian Madgwick. An efficient orientation filter for inertial and inertial / magnetic sensor arrays. *undefined*, 2010.

[19] David C. Van Metre, John R. Wenz, and Franklyn B. Garry. Lameness in Cattle:. *American Association of Bovine Practitioners Conference Proceedings*, pages 40–43, September 2005.

[20] Andrew S. Monaghan, Jessie M. Huisinga, and Daniel S. Peterson. The application of principal component analysis to characterize gait and its association with falls in multiple sclerosis. *Scientific Reports*, 11(1):12811, December 2021.

[21] NZIER. New Zealand Dairy Statistics, November 2017.

[22] Karl Pearson. LIII. On lines and planes of closest fit to systems of points in space. *The London, Edinburgh, and Dublin Philosophical Magazine and Journal of Science*, 2(11):559–572, November 1901. Publisher: Taylor & Francis _eprint: https://doi.org/10.1080/14786440109462720.

[23] Jan K. Shearer, Sarel R. Van Amstel, and Bruce W. Brodersen. Clinical diagnosis of foot and leg lameness in cattle. *The Veterinary Clinics of North America. Food Animal Practice*, 28(3):535–556, November 2012.

[24] P. T. Thomsen, L. Munksgaard, and F. A. Tøgersen. Evaluation of a Lameness Scoring System for Dairy Cows. *Journal of Dairy Science*, 91(1):119–126, January 2008.

[25] M. Tijssen, F. M. Serra Braganca, K. Ask, M. Rhodin, P. H. Andersen, E. Telezhenko, C. Bergsten, M. Nielen, and E. Hernlund. Kinematic gait characteristics of straight line walk in clinically sound dairy cows. *PLOS ONE*, 16(7):e0253479, July 2021. Publisher: Public Library of Science.

[26] D. A. Winter and H. J. Yack. EMG profiles during normal human walking: stride-to-stride and inter-subject variability. *Electroencephalography and Clinical Neurophysiology*, 67(5):402–411, November 1987.